Electronic Supporting Information

Structural Insights to Metal Ion Linked Multilayers on Metal Oxide Surfaces via Energy Transfer and Polarized ATR Measurements

Ashley Arcidiacono,[a] Cory Ruchlin,[b] Grace M. McLeod,[a] Dhruba Pattadar,[c] Sarah Lindbom,[a] Alex J. Robb,[a] Suliman Ayad,[a] Nikolas R. Dos Santos,[a] Igor V. Alabugin,[a] S. Scott Saavedra,[c] Kenneth Hanson[a]

[a]Department of Chemistry and Biochemistry, Florida State University, Tallahassee, Florida 32306, United States

[b]Department of Chemistry, McGill University, 801 Sherbrooke Street West, Montreal, Quebec, Canada H3A 0B8

[c]Department of Chemistry and Biochemistry, University of Arizona, Tucson, Arizona 85721, United States

Contents

Synthesis:

Platinum(II) meso-mono(3-carboxyphenyl)-tris(2,4-ditertbutylphenyl)porphine (P1):

P1 was synthesized using a procedure modified from literature.[1] To a 1000 mL round bottom flask flame dried under vacuum, anhydrous dichloromethane (600 mL) was added and deaerated by bubbling with N_2 for 30 minutes. Methyl 4-formyl benzoate (0.500 g, 3.046 mmol, 1 eq) and 3,5-ditertbutyl benzaldehyde (1.995 g, 9.137 mmol, 3 eq) were added and the solution was stirred for 15 minutes. Pyrrole (0.845 mL, 12.183 mmol, 4 eq) was injected followed by boron trifluoride diethyl etherate (0.094 mL, 0.761 mmol, 0.25 eq). The reaction was allowed to proceed in darkness for 3 hours. After 3 hours, 2,3-dichlororo-5,6-dicyano-1,4-benzoquinone (0.519 g, 2.284 mmol, 0.75 eq) was added and the reaction was stirred for one additional hour. The crude mixture was prepared for dry loading on a flash column by rotary evaporation of the reaction mixture with 30 g silica gel. This was flashed over a silica plug with $CHCl_3$ until eluent ran colorless. The resulting solution of purple, crude product was rotary evaporated with 4 g silica gel for dry loading on subsequent flash column. Esterified porphyrin was isolated via flash chromatography (silica gel wet packed in 40:60, DCM:hexanes; dry loaded silica/crude product; eluted using 40:60, DCM:Hexanes until collection of first fraction, followed by 50:50, DCM:Hexanes for subsequent fractions) to yield 0.334 g (10.9%).

The isolated esterified porphyrin (0.307 g, 0.304 mmol, 1 eq) was platinated by dissolving in benzonitrile (30 mL), adding $PtCl_2$ (200 mg, 0.752 mmol, 2.5 eq), and refluxing for two hours. Upon completion of reaction, solvent was distilled off to isolate crude product. Pure platinated porphyrin was obtained via flash chromatography (silica wet packed in 30:70, DCM:Hexanes; dry loaded crude/silica gel; eluted with 30:70, DCM:Hexanes) to yield 0.292 g (80%). The product's identity was confirmed via ^{1}H NMR and comparison to previously published data.[1]

Platinated, ester protected porphyrin (0.292 g, 0.243 mmol, 1 eq) was then dissolved in 50:50:5, ethanol:THF:water (total volume 26.25 mL) and KOH (0.3 g) was added. The mixture was refluxed overnight. Concentrated HCl was added (~4 drops) and stirred for five minutes to ensure protonation and the red-orange product was isolated from suspension by centrifugation to yield 0.278 g (96%). ^{1}H NMR (700 MHz, $CDCl_3$): δ (ppm) 9.15 (s, 1H), 9.16 (d, 4H), 9.05 (d, 2H), 8.56 (d, 2H), 8.45 (d, 2H), 7.87 (m, 6H), 7.51 (m, 4H), 1.55 (s, 54H). ^{13}C NMR (176 MHz, $CDCl_3$): δ (ppm) 169.3 (1C), 148.6 (2C), 147.5 (1C), 145.6 (6C), 140.5 (2C), 134.5 (2C), 133.1 (2C), 132.7 (3C), 132.0 (1C), 130.2 (2C), 129.5 (1C), 128.2 (2C), 126.0 (2C), 123.7 (3C), 122.6 (4C), 119.5 (6C), 118.2 (2C), 113.1 (2C), 103.6 (1C), 35.1 (6C), 31.7 (18C). LCMS (ESI^+) m/z: $[M + H]^+$ Calculated for $C_{69}H_{76}N_4O_2Pt$ 1187.56; Found 1187.56012.

Platinum (II) 4'-(10,15,20-tris(3,5-di-*tert*-butylphenyl)porphyrin-5-yl)-[1,1'-biphenyl]-4-carboxylic acid (P2):

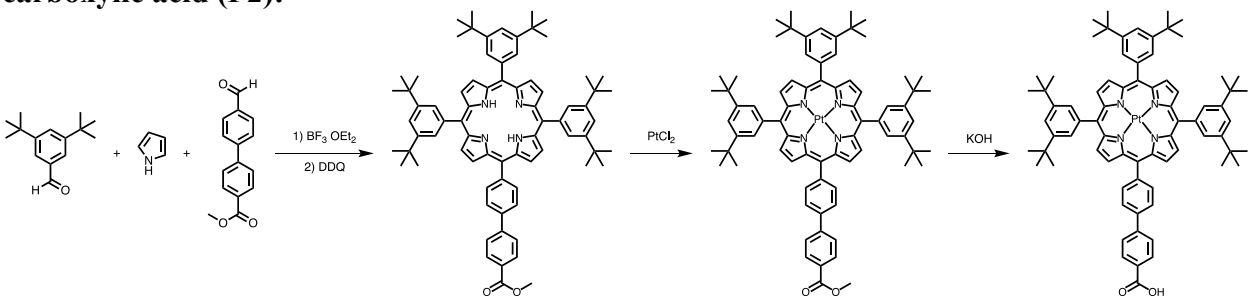

P2 was synthesized following a similar procedure to **P1** with minor modification. A 500 mL three neck round bottom flask was flame dried under vacuum and backfilled with N_2 prior to use. Anhydrous dichloromethane (220 mL) was added and degassed by sparging with N_2 for 30 minutes. Under a stream of N_2, methyl-4(4-formylphenyl) benzoate (0.268 g, 1.12 mmol, 1 eq) and 3,5-ditertbutyl benzaldehyde (0.731 g, 3.35 mmol, 3 eq) were added. This mixture was stirred for fifteen minutes prior to the injection of pyrrole (0.31 mL, 4.46 mmol, 4 eq). After stirring again for fifteen minutes, boron trifluoride diethyl etherate was added (0.034 mL, 0.23 mmol, 0.25 eq) and the reaction was allowed to proceed in darkness for three hours. Following three hours of stirring, 2,3-Dichloro-5,6-dicyano-1,4-benzoquinone was added (0.190 g, 0.84 mmol, 0.75 eq) and the reaction mixture was stirred overnight. The reaction mixture was rotary evaporated with 4 g silica gel and flashed over a silica plug with $CHCl_3$ until colorless eluent to isolate crude porphyrin. The unsymmetric, esterified porphyrin was purified via flash chromatography (dry load crude/silica gel; wet packed and eluted with 40:60, hexanes:chloroform) and identified by its red fluorescence on TLC (141 mg, 11.6% yield).

To platinate the isolated porphyrin, $PtCl_2$ (84 mg, 0.316 mmol, 2.5 eq) was dissolved in benzonitrile (12.6 mL), heated to 100°C, and allowed to stir for one hour. Porphyrin (140 mg, 0.129 mmol, 1 eq) was added; the reaction mixture was refluxed for three hours. Complete platination was confirmed by UV Vis prior to use in subsequent synthetic step. Benzonitrile was distilled off. Crude product was prepared for dry loading by dissolving in DCM and rotary evaporating with 1 g silica gel. Flash chromatography was used to purify the platinated porphyrin (dry load crude/silica gel, wet packed and eluted with 30:70, DCM:hexanes) and product collected by rotary evaporation (139 mg, 84% yield).

Platinated porphyrin (100 mg, 0.078 mmol, 1 eq) was then dissolved in 50:50:5, ethanol:THF:water (total volume 26.25 mL) and KOH was added (0.3 g, 5.35 mmol, 0.69 eq). The mixture was refluxed overnight. Concentrated HCl was added to pH=3 and the solution stirred for five minutes to ensure protonation; the resulting red-orange product was isolated from suspension by centrifugation (96 mg, 97%). ^{1}H NMR (700 MHz, $CDCl_3$): δ (ppm) 8.86 (d, 8H), 8.42 (s, 4H), 8.31 (d, 4H), 8.28 (s, 4H), 8.02 (d, 2H), 7.77 (t, 2H), 7.41 (s, 1H), 7.11 (s, 2H), 6.56 (s, 1H), 6.51 (s, 1H), 1.54 (s, 54H). ^{13}C NMR (176 MHz, $CDCl_3$): δ (ppm) 148.9 (6C), 146.1 (2C), 141.1 (4C), 140.5 (6C), 134.5 (6C), 131.1 (4C), 129.01 (8C), 127.6 (6C), 125.7 (3C), 123.6 (2C), 121.1 (8C), 35.1 (6C), 31.8 (18C). LCMS (ESI$^+$) m/z: $[M + H]^+$ Calculated for $C_{75}H_{80}N_4O_2Pt$ 1263.59; Found 1263.59449.

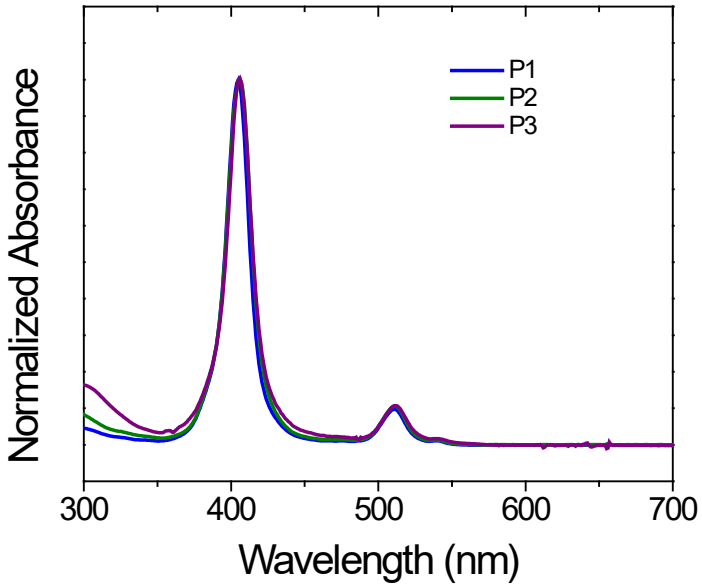

Figure S1. Absorbance spectra of **P1-3** in chloroform:methanol (1:1, v/v).

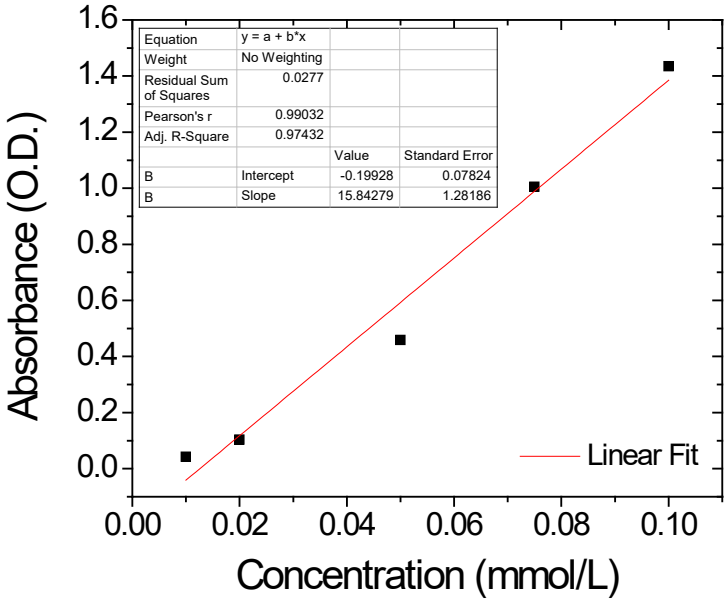

Figure S2. Extinction coefficient determination of **P1** chloroform:methanol (1:1, v/v).

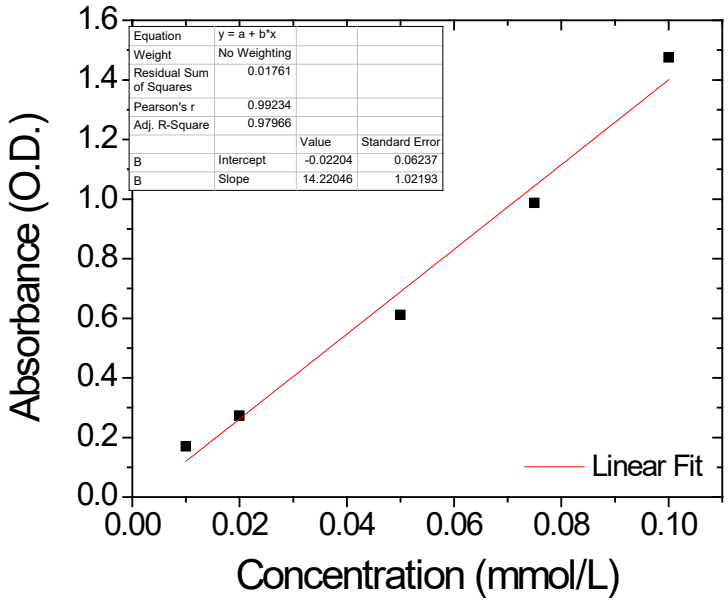

Figure S3. Extinction coefficient determination of **P2** in 1:1 chloroform:methanol.

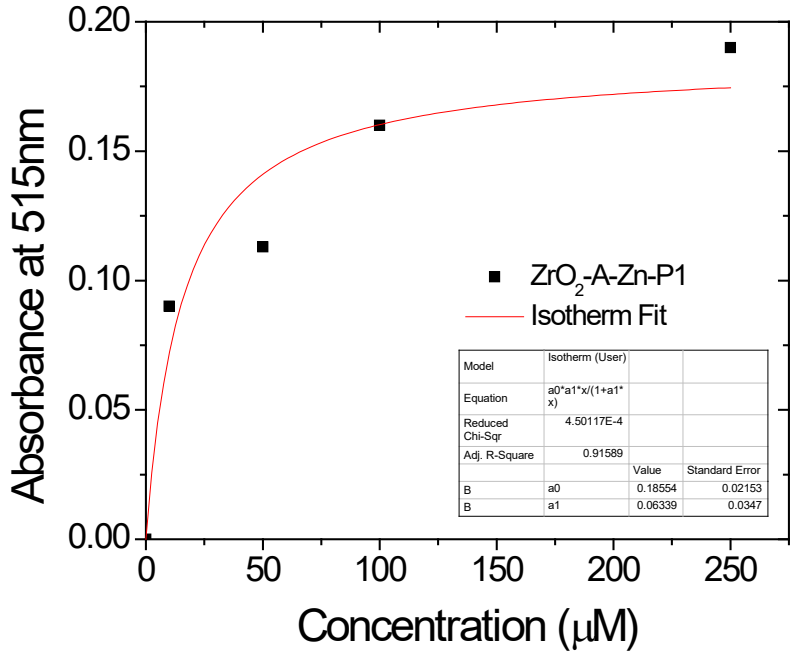

Figure S4. Adsorption isotherm of **P1** on ZrO_2-**A**-Zn with respect to the **P1** loading solution concentration (1:1, chloroform:methanol).

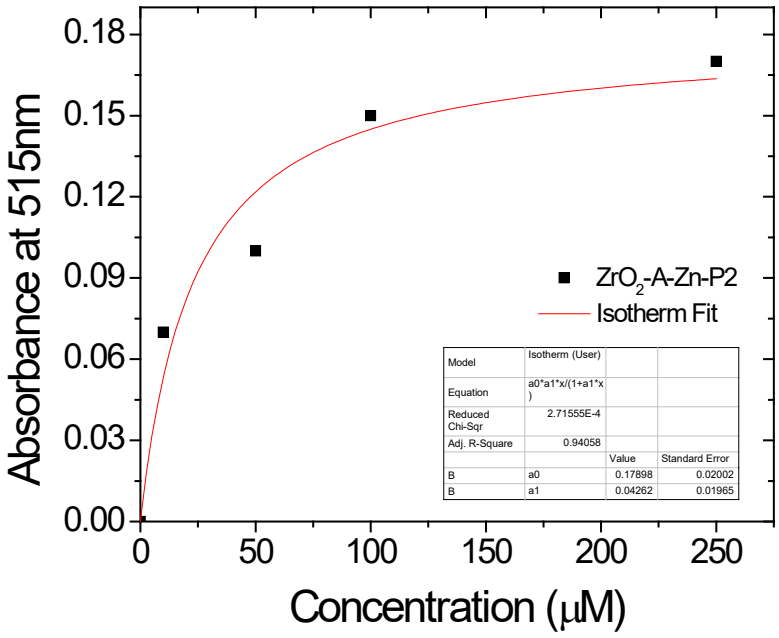

Figure S5. Adsorption isotherm of **P2** on ZrO_2-**A**-Zn with respect to the **P2** loading solution concentration (1:1, chloroform:methanol).

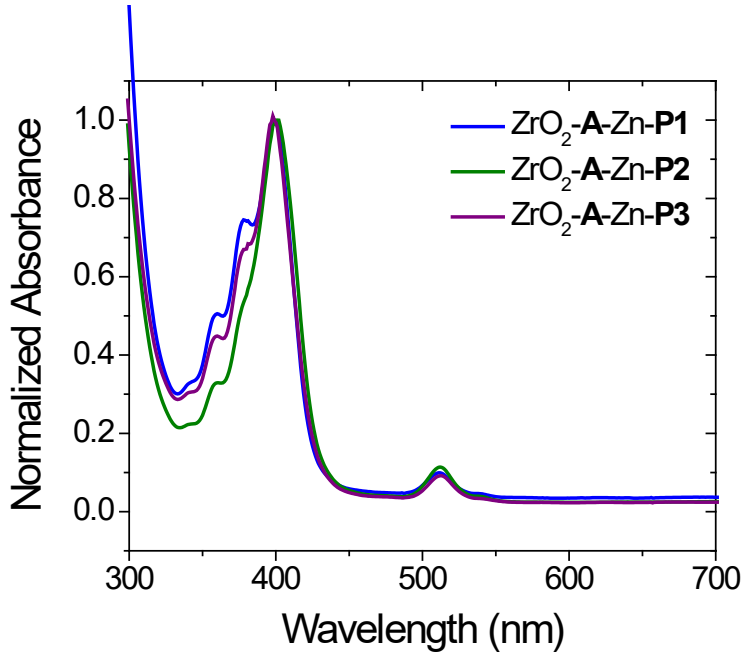

Figure S6. Absorption spectra of ZrO_2-**A**-Zn-**PX** films.

Table S1. Fit parameters for the emission decay of ZrO_2-**A** and ZrO_2-**A**-Zn-**P3** in MeCN at 460 nm (λ_{ex} = 360 nm)**.**

	A_1	τ_1 (ns)	A_2	τ_2 (ns)	<τ> (ns)
ZrO_2-**A**	0.6	1.1±0.1	0.4	6.2±0.2	5.1±0.2
ZrO_2-**A**-Zn-**P3**	0.8	1.0±40.2	0.2	4.7±0.8	3.1±0.3

Table S2. Fit parameters and weighted average lifetimes for the first 300 ps of the transient absorption kinetics at 460 nm for ZrO_2-**A**-Zn-**P1**, ZrO_2-**A**-Zn-**P2**, and ZrO_2-**A**-Zn-**P3** in MeCN (λ_{ex} = 360 nm).

	A_1	τ_1 (ps)	A_2	τ_2 (ps)	<τ> (ps)
ZrO_2-**A**-Zn-**P1**	0.16	8±4	0.84	40±11	39±11
ZrO_2-**A**-Zn-**P2**	0.16	8±3	0.84	43±5	41±4
ZrO_2-**A**-Zn-**P3**	0.09	19±6	0.91	180±55	180±54

Table S3. Fit parameters and weighted average lifetimes of emission at 670 nm for ZrO_2-**PX** and ZrO_2-**A**-Zn-**PX** (λ_{ex}=512 nm).

Sample	A_1	τ_1 (µs)	A_2	τ_2 (µs)	<τ> (µs)	TET rate ($\times 10^3$ s^{-1})
ZrO_2- **P1**	0.81	52 ± 4	0.19	14 ± 5	49±4	
ZrO_2-**P2**	0.85	52 ± 3	0.15	10 ± 2	50±2	
ZrO_2-**P3**	0.72	40 ± 8	0.28	56 ± 10	52±3	
ZrO_2-**A**-Zn-**P1**	0.38	42 ± 4	0.62	12 ± 2	33±4	9.8±0.6
ZrO_2-**A**-Zn-**P2**	0.84	57 ± 7	0.16	28 ± 4	36±2	7.0±0.3
ZrO_2-**A**-Zn-**P3**	0.84	72 ± 6	0.16	25 ± 7	42±5	4.5±0.8

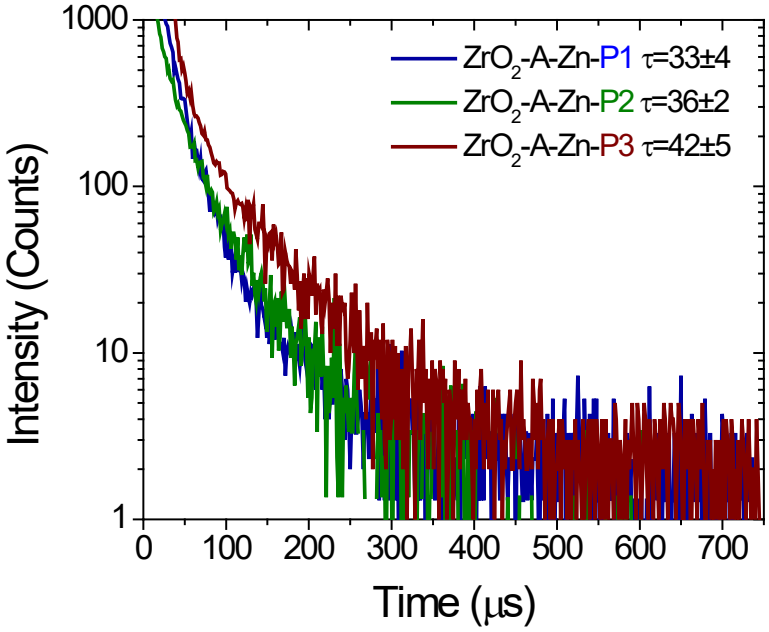

Figure S7. Time-resolved emission decays at 670 nm for ZrO_2-**A**-Zn-**PX** films in N_2 deaerated MeCN (λ_{ex}=512 nm).

Table S4. Fit parameters and weighted average lifetimes of emission at 460 nm for ZrO_2-**A** and ZrO_2-**A**-Zn-**P3** on planar (p-) and mesoporous (m-) substrates in MeCN (λ_{ex} = 360 nm).

	A_1	**τ_1 (ns)**	**A_2**	**τ_2 (ns)**	**$\langle\tau\rangle$ (ns)**	**k_{FRET} ($\times10^8$ s^{-1})**
p-ZrO_2-**A**	0.6	1.1±0.1	0.4	6.2±0.2	5.1±0.2	-
m-ZrO_2-**A**	0.2	1.9±0.2	0.8	6.8±0.7	6±1	-
p-ZrO_2-**A**-Zn-**P3**	0.8	0.8±0.1	0.2	5.1±0.1	3.5±0.5	1.0±0.4
m-ZrO_2-**A**-Zn-**P3**	0.8	1.0±40.2	0.2	4.7±0.8	3.1±0.3	1.3±0.1

Table S5. ATR experimental conditions.

Species	**Injection concentration (μM)**	**Solvent and flush solvent**	**Incubation time (min)**	**Wavelength Integration range (nm)**
A	40	Ethanol	60	350-420
Zn	500	Ethanol	60	350-420
P1, P2, and P3	100	Blank – ethanol; Adsorption from chloroform/ methanol (50-50 %); Flush - chloroform/ methanol (50-50 %); then ethanol	60	480-550

Table S6. Mean tilt angle and surface coverage as determined by p-ATR of ZrO_2-**A**-Zn-**P1**. All values are the average of three independent trials with standard deviations reported as the error.

Species	**Mean tilt angle (°)**	**Surface coverage (mol/cm^2)**
A	30 ± 1.0	$3.1 \times 10^{-10} \pm 2.4 \times 10^{-11}$
A at (**A**-Zn)	35 ± 3	
A at (**A**-Zn-**P1**)	37 ± 3	
P1 at (**A**-Zn-**P1**)	50 ± 1	$2.8 \times 10^{-11} \pm 9.4 \times 10^{-12}$

Table S7. Mean tilt angle and surface coverage as determined by p-ATR of ZrO_2-**A**-Zn-**P2**. All values are the average of three independent trials with standard deviations reported as the error.

Species	**Mean tilt angle (°)**	**Surface coverage (mol/cm^2)**
A	30 ± 2	$3.6 \times 10^{-10} \pm 5.8 \times 10^{-11}$
A at (**A**-Zn)	32 ± 3	
A at (**A**-Zn-**P2**)	36 ± 3	
P1 at (**A**-Zn-**P2**)	36 ± 2	$4.6 \times 10^{-11} \pm 2.1 \times 10^{-11}$

Table S8. Mean tilt angle and surface coverage as determined by p-ATR of ZrO_2-**A**-Zn-**P3**. All values are the average of three independent trials with standard deviations reported as the error.

Species	**Mean tilt angle (°)**	**Surface coverage (mol/cm^2)**
A	33 ± 3	$4.3 \times 10^{-10} \pm 6.1 \times 10^{-11}$
A at (**A**-Zn)	38 ± 1	
A at (**A**-Zn-**P3**)	39 ± 1	
P1 at (**A**-Zn-**P3**)	22 ± 4	$3.1 \times 10^{-11} \pm 1.8 \times 10^{-11}$

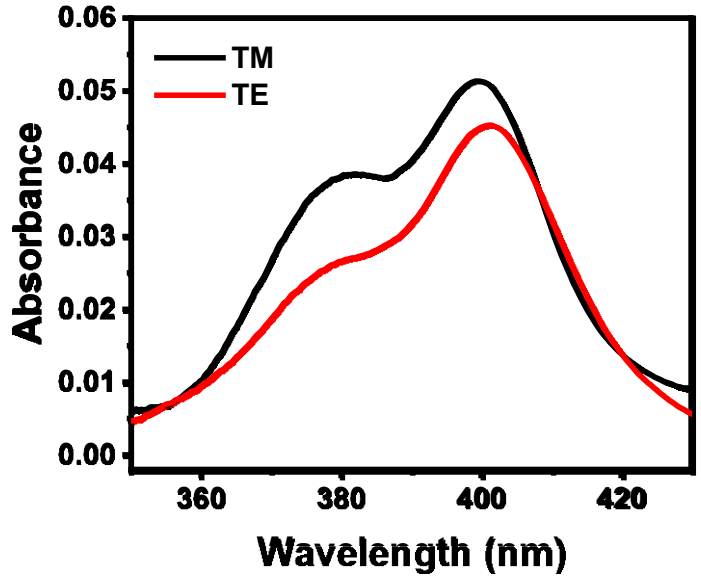

Figure S8. ATR spectra of 405 NHS ester-poly(lysine) on TFD ITO.

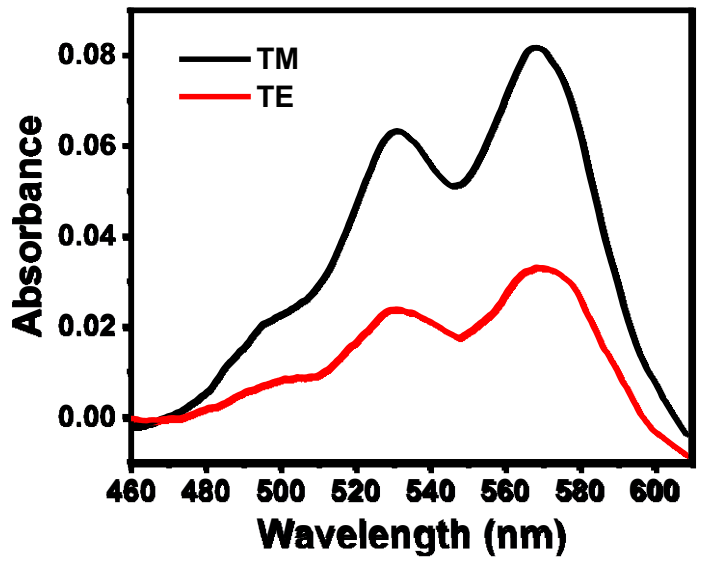

Figure S9. ATR spectra Rhodamine B-dextran on TFD ITO.

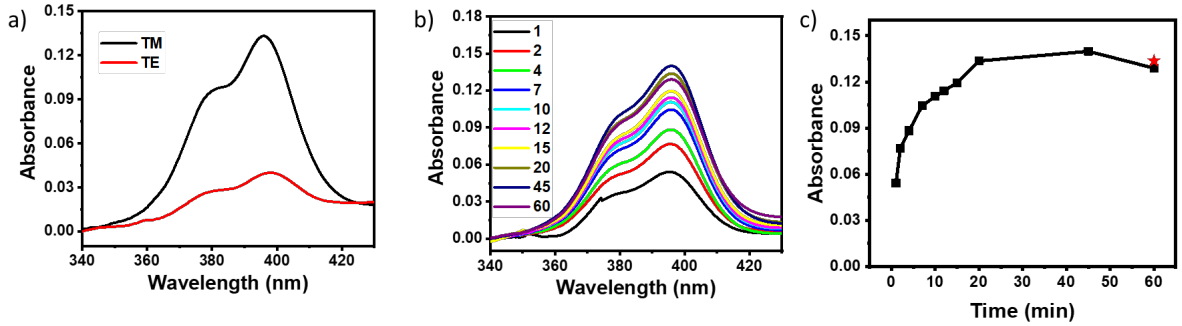

Figure S10. ATR spectra of **A** in ZrO_2-**A** on TFD ITO (a) and monitored loading over 60 minutes (b) with the resulting isotherm (c). The red star indicates the absorbance after flushing the cell with solvent.

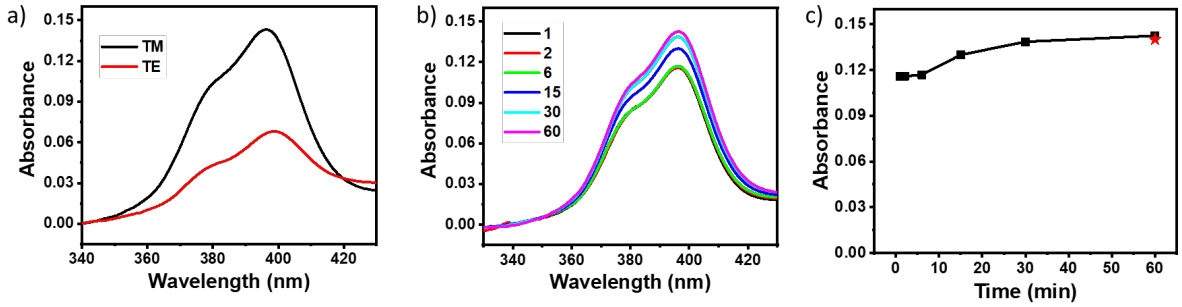

Figure S11. ATR spectra of **A** in ZrO_2-**A**-Zn on TFD ITO (a) and monitored loading over 60 minutes (b) with the resulting isotherm (c). The red star indicates the absorbance after flushing the cell with solvent.

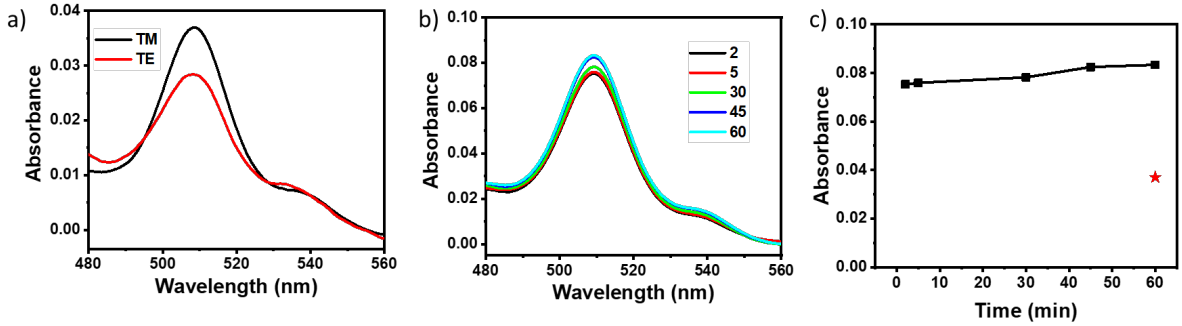

Figure S12. ATR spectra of **P1** in ZrO_2-**A**-Zn-**P1** on TFD ITO (a) and monitored loading over 60 minutes (b) with the resulting isotherm (c). The red star indicates the absorbance after flushing the cell with solvent.

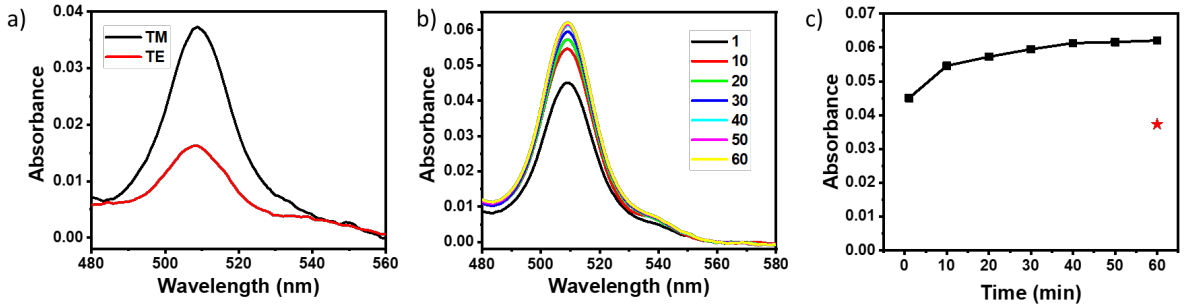

Figure S13. ATR spectra of **P2** in ZrO_2-**A**-Zn-**P2** on TFD ITO (a) and monitored loading over 60 minutes (b) with the resulting isotherm (c). The red star indicates the absorbance after flushing the cell with solvent.

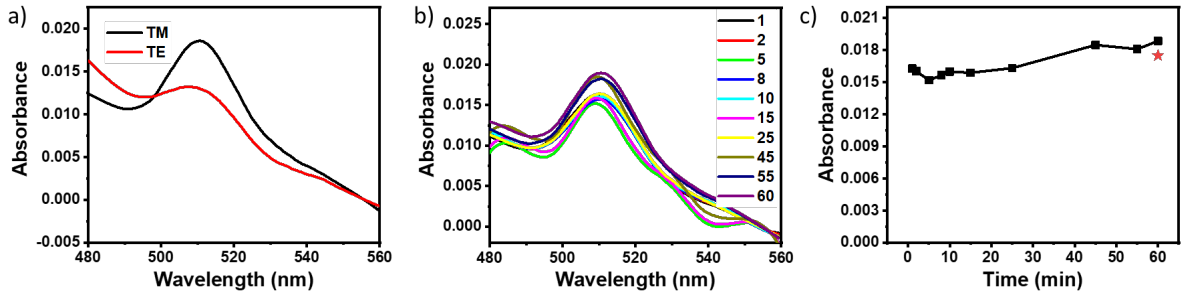

Figure S14. ATR spectra of **P3** in ZrO_2-**A**-Zn-**P3** on TFD ITO (a) and monitored loading over 60 minutes (b) with the resulting isotherm (c). The red star indicates the absorbance after flushing the cell with solvent.

Geometry calculations

To determine the potential orientations of the bilayer components which would correspond to the experimental FRET efficiency, a simplified model of the bilayer systems was constructed and used as a basis for the geometric components of the efficiency calculations, as described in the manuscript. Under the simplified assumptions that **A** is oriented at a fixed angle (θ_A) to the surface normal, as determined by p-ATR, and that the Zn-ion acts as a rigid vertex around which **PX** can freely rotate, we set the Zn linker ion is set as the origin of coordinates, surface normal as as the z-axis, and the vector representation of **A** (r_A) in the x,z-plane. In spherical polar space, the free motion of the vector model for **PX** (r_P) can be described as a combination of azimuthal (φ) and altitudinal (θ_P) rotations, yielding the full traceable sphere depicted in Figure 7 of the main paper. The lengths of r_A and r_P were extracted from the gas-phase optimized geometries of the organic components, calculated at the B3LYP/6-31G(d) level of theory (Figure 7a, Table S10). The distances are measured between a Zn atom, placed without further optimization based on previously reported coordination bonds lengths,[2,3] and the molecular centroids (in Figure 7, the vectors shown correspond to the lengths of the full molecules for clarity, and the centroids are marked with circles). The lengths of these vectors, along with all the experimental parameters used in these calculations are listed in Table S9.

As mentioned, any coordinate ($|r_P|$,θ_P,φ) adopted by r_P must be accompanied by one of two axial rotations (θ_{rot}), corresponding to a clockwise or anticlockwise dihedral rotation about the meso-axis of **PX**, such that the minimum angle (θ_{plane}) between the plane of the porphyrins macrocycle and surface normal is consistent with the plane angle found by p-ATR (θ_{tilt}). Knowledge of the θ_{rot} is necessary due to the multiple degenerate transition dipoles of **PX** being oriented along the plane. To account for this, the plane of the **PX** macrocycle was modelled by the shared plane (**Q**) of an axial (μ_1) and transverse (μ_2) vector propagating from the centroid point at the tip of r_P. These were defined such that $\mu_1 \| r_P$ and $\mu_2 \perp r_P$, and $|\mu_1|=|\mu_2|=1$. Given that θ_{plane} is defined as the angle between surface normal (basis vector k) and the maximum gradient of **Q**, two corollaries follow: 1) any position where $\theta_P < \theta_{tilt}$ or $\theta_P > 180°-\theta_{tilt}$ can be immediately discarded, since any value of θ_{rot} will result in a $\theta_{plane} < \theta_{tilt}$, and 2) the maximum gradient of **Q** will be orthogonal to the normal vector (N) of **Q** (Figure S15a). For determination of the relationship between θ_{plane} , θ_P, and θ_{rot}, we transformed into cartesian space and use the vector components of μ_2 (μ_1 is independent of θ_{rot}).

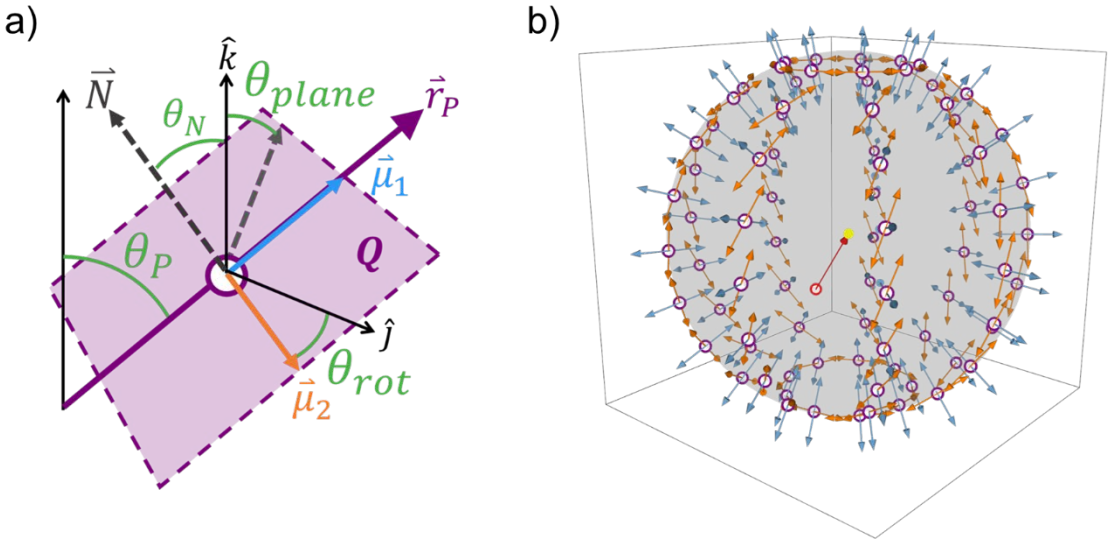

Figure S15. (a) Geometric depiction of porphyrin plane (**Q**), axial and transverse vectors (μ_1 and μ_2), maximum gradient (light grey), plane normal (N) and the relevant angles (b) spatial distribution of positive and negative μ_1 (blue) and μ_2 (orange) vectors propagating from r_P centroids (purple circles) across zone corresponding to points which would satisfy $\theta_{plane}=\theta_{tilt}$. For clarity, plot is shown at low sampling resolution, μ vectors are magnified by 4, and only μ_2 corresponding to clockwise θ_{rot} is shown.

Defining θ_{rot} as the angle between μ_2 and the vector perpendicular to r_P in the x,y-plane, the cartesian components of μ_2 at a given spherical polar coordinate ($|r_P|$,θ_P,φ) and θ_{rot} were given by:

$$\mu_{2x} = -\sin\theta_{rot}\cos\theta_P\cos\phi - \cos\theta_{rot}\sin\phi \qquad (a)$$
$$\mu_{2y} = \cos\theta_{rot}\cos\phi - \sin\theta_{rot}\cos\theta_P\sin\phi \qquad (b)$$
$$\mu_{2z} = \sin\theta_{rot}\sin\theta_P \qquad (c)$$

We then defined μ_1 as the unit vector parallel to r_P:

$$\mu_{1x} = \sin\theta_P \cos\phi \quad (d)$$
$$\mu_{1y} = \sin\theta_P \sin\phi \quad (e)$$
$$\mu_{1z} = \cos\theta_P \quad (f)$$

Since μ_1 and μ_2 are orthonormal, their cross product gives N, the unit vector normal to **Q:**

$$\vec{N} = \vec{\mu}_1 \times \vec{\mu}_2 \quad (g)$$

Implicitly, N is orthogonal to all vectors in **Q**, and therefore, the angle (θ_N) between N and the basis vector in the z-direction (k) is complimentary to θ_{plane}:

$$\vec{N} \cdot \hat{k} = \cos\theta_N = \cos\left(\frac{\pi}{2} - \theta_{plane}\right) = \sin\theta_{plane} \quad (h)$$

By combining equations g and h we get that:

$$\sin\theta_{plane} = (\vec{\mu}_1 \times \vec{\mu}_2) \cdot \hat{k} = \mu_{1x}\mu_{2y} - \mu_{2x}\mu_{1y} \quad (i)$$

Following substitution using equations a-f, this simplifies to:

$$\sin\theta_{plane} = \sin\theta_P \cos\theta_{rot} \quad (j)$$

Thus, the value of θ_{rot} which describes bilayer geometries consistent with θ_{tilt} determined by p-ATR is dependent solely on θ_P and could be determined by rearrangement and substitution of equation j, to provide the restriction:

$$\theta_{rot} = \arccos\left(\frac{\sin\theta_{tilt}}{\sin\theta_P}\right) \quad (k)$$

From here, we superimposed the transition dipole moments onto the reduced set of geometries. Given that the magnitudes of the transition dipoles are irrelevant to the calculation of the FRET efficiency in this framework, the transition dipole of **A** was modelled by r_A, as the transition dipole moment is known to be parallel to the C-9,C-10-axis of the anthracene molecule.[4] Additionally, while the true transition dipoles of **PX** are known to point along the N-N axes,[5] a later step in which we calculated the average orientation factor ($\langle\kappa^2\rangle$) would provide equivalent results for any pair of perpendicular vectors that lie within **Q**. For convenience, we used μ_1 and μ_2 to stand in for the dipole moments. The geometric arrangement of all the surrogate dipole vectors across the restricted space is shown in Figure S15b.

With the dipole vectors oriented in space, we then calculated a theoretical value for the FRET efficiency (E_{theo}) at every possible position on the surface of the spherical section. E_{theo} is calculated from equations 1-3 in the main paper, reproduced below:

$$E = \frac{1}{1 + \left(\frac{r_{DA}}{R_0}\right)^6} \quad (l)$$

$$R_0 = 9780(\kappa^2 \Phi_D n^{-4} J)^{1/6} \qquad (m)$$

$$\kappa^2 = (\cos\alpha - 3\cos\beta\cos\gamma)^2 \qquad (n)$$

The intermolecular distance (r_{DA}) is given by the magnitude of the vector (v_{DA}) between the molecular centroids at each position, Φ_D, n, and J are empirically derived experimental parameters, and κ^2 is calculated from the angles (α, β, and γ) between the surrogate dipole vectors. In equation n, α is the angle between the transition dipole of **A** (r_A) and v_{DA}, β is the angle between the transition dipole of **PX** (μ_1,μ_2) and v_{DA}, and γ is the angle between the two molecules' transition dipoles. Since there are two degenerate transition dipoles for **PX**, there are two values for both β and γ. Thus, we calculate two values for κ^2 using both μ_1 and μ_2 as the dipole moment for **PX** and take their average as the orientation factor ($\langle\kappa^2\rangle$):[6]

$$\langle\kappa^2\rangle = \frac{\kappa_1^2 + \kappa_2^2}{2} \qquad (o)$$

where κ_1^2 and κ_2^2 are the orientation factor calculated using μ_1 and μ_2 as the **PX** dipole, respectively.

Table S9. Length and experimental parameters used in geometric modelling.

	$\lvert r_A \rvert$ (Å)	θ_A (°)	$\lvert r_P \rvert$ (Å)	θ_{tilt} (°)	E_{exp}	Φ_D	n	J
A-Zn-**P1**	9.26	37	11.4	50	0.994	0.53	1.36	2×10^{-14}
A-Zn-**P2**		36	15.8	36	0.993			
A-Zn-**P3**		39	20.2	22	0.973			

Using $\langle\kappa^2\rangle$, we then calculated E_{theo} at each possible position adoptable by r_P in the model. The resulting surfaces are shown in Figure S16a-c. As mentioned above, the restrictions on the adoptable space are satisfied by both clockwise and anticlockwise axial rotation by θ_{rot}, corresponding to the mirror image of the E_{theo} surface reflected across the x,z-plane.

To finally determine the geometries which are most consistent with the experimentally determined FRET efficiency (E_{exp}), we first truncate the surface to only the segment above the x,y-plane, removing extraneous points where steric interactions with the layers below would prevent **PX** from adopting the position. A heatmap showing the absolute difference between E_{theo} and E_{exp} was then constructed. To account for the multiple θ_{rot} values possible, the mirror image of the heatmap was additionally superimposed and the minimum difference value was retained at each point, yielding the surfaces in Figure S16d-i.

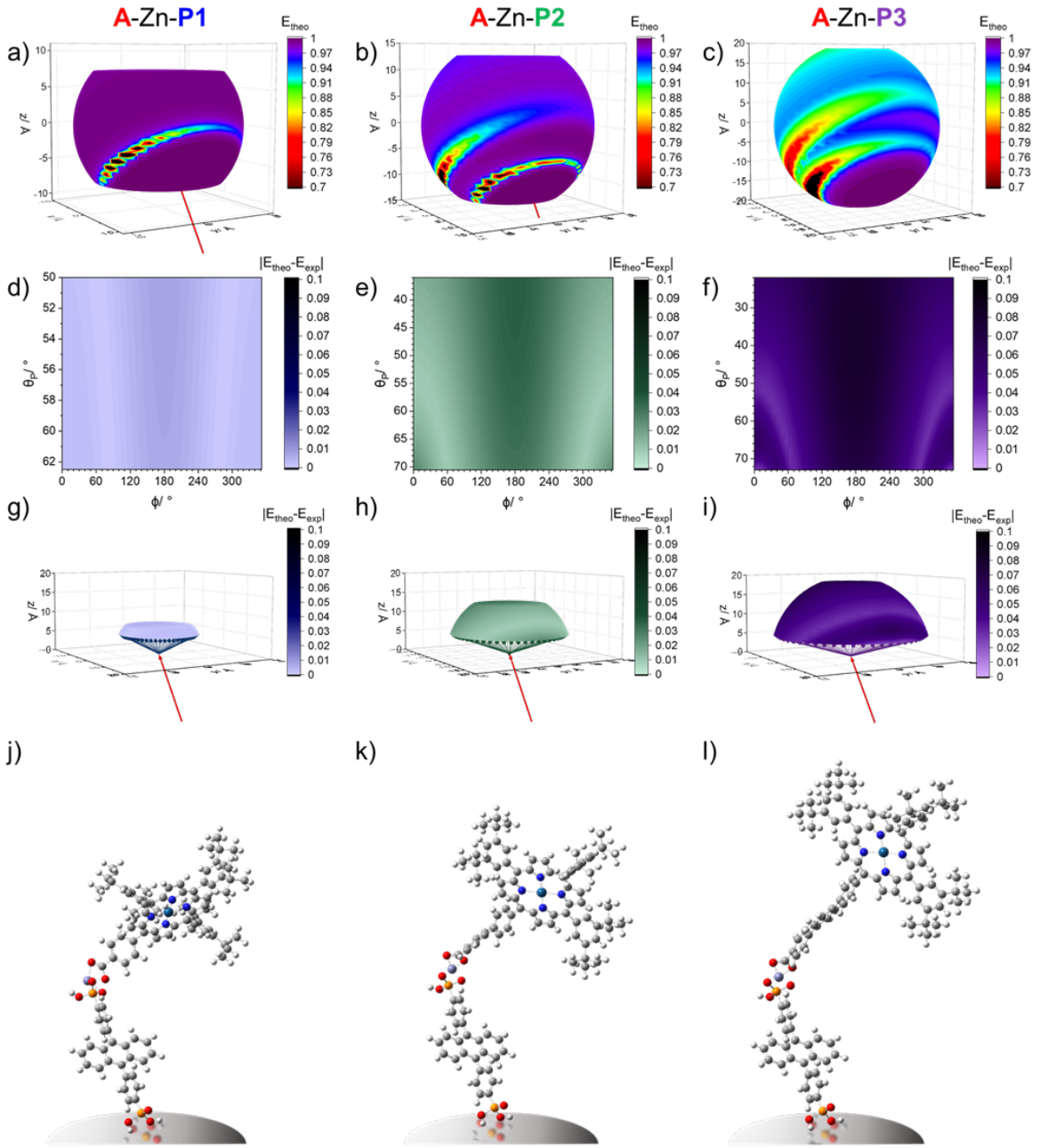

Figure S16. Surfaces showing E_{theo} calculated at each point along the possible orientation space of the **A**-Zn-**P1** (a), **A**-Zn-**P2** (b), and **A**-Zn-**P3** (c) bilayers, calculated at a coverage resolution of 2601 points. Red vectors show orientation of fixed **A** molecule. (d-f) Surfaces showing absolute difference between E_{theo} and E_{exp}, with respect to the angle parameters, θ_P and φ and (g-i) projected onto truncated spherical sections. (j-l) Molecular depictions of orientations in "hotspot" regions of good agreement between E_{theo} and E_{exp}.

Table S10. DFT Optimized Atomic Coordinates for **A**, **P1**, **P2**, and **P3.** Pt and **A** centroid (Bq) placed at molecular centroid without further optimization. Zn atoms placed at distance to coordinating O's based on previously reported calculations/crystallography.[2,3]

A, Total Energy (excluding Bq and Zn) = -2137.019987 Hartree			
C	-0.7134	3.668	0.0242
C	0.7087	3.6689	0.0446
C	1.4003	2.4872	0.0497
C	0.7224	1.2247	0.036
C	-0.7242	1.2237	0.0311
C	-1.4035	2.4853	0.0183
C	1.4265	0.001	0.0331
C	0.7242	-1.2237	0.0312
C	-0.7225	-1.2247	0.036
C	-1.4265	-0.001	0.0331
C	1.4035	-2.4853	0.0184
C	0.7134	-3.668	0.0244
C	-0.7087	-3.669	0.0448
C	-1.4003	-2.4872	0.0499
C	-2.9242	-0.0029	0.0311
C	2.9242	0.0029	0.0311
C	3.6367	0.1584	-1.1696
C	5.0291	0.1625	-1.178
C	5.7379	0.0134	0.0227
C	5.0373	-0.1439	1.2249
C	3.6427	-0.1487	1.2256
C	-3.6367	-0.1587	-1.1695
C	-5.0291	-0.1628	-1.1779
C	-5.7379	-0.0133	0.0228
C	-5.0373	0.1442	1.2249
C	-3.6427	0.149	1.2256
P	-7.5355	0.0035	0.0766
O	-8.125	0.2213	1.4215
O	-7.8868	-1.3775	-0.6964
O	-8.0393	1.1018	-1.0264
P	7.5354	-0.0034	0.0766
O	8.125	-0.221	1.4215
O	7.8869	1.3774	-0.6967
O	8.0392	-1.1021	-1.0262
H	-1.2524	4.6114	0.0147
H	1.2466	4.613	0.056
H	2.4845	2.4952	0.066
H	-2.4877	2.4914	0.0037
H	2.4877	-2.4914	0.0038
H	1.2524	-4.6115	0.0149
H	-1.2466	-4.613	0.0562
H	-2.4845	-2.4953	0.0662
H	3.0894	0.2758	-2.1006
H	5.5631	0.2839	-2.1157
H	5.5912	-0.2567	2.1518
H	3.1024	-0.268	2.1605
H	-3.0894	-0.2763	-2.1006
H	-5.5631	-0.2844	-2.1156
H	-5.5911	0.2573	2.1517
H	-3.1024	0.2685	2.1605
H	-8.8483	-1.5001	-0.7797
H	-8.3605	1.893	-0.5621

H	8.3607	-1.893	-0.5615
Zn	9.2616	0.0922	-0.1442
Bq	0	0	0.0331

P1, Total Energy (excluding Pt and Zn) = -3045.852853 Hartree			
N	1.4393	2.0991	-0.0743
N	-1.4889	1.9806	-0.0229
N	-1.4678	-0.9592	-0.0133
N	1.4611	-0.8381	-0.0219
C	2.7988	1.8799	-0.078
C	3.4173	3.1733	-0.1135
C	2.4288	4.1206	-0.1214
C	1.1622	3.4462	-0.1103
C	-0.1131	4.0359	-0.1327
C	-1.3396	3.3351	-0.1147
C	-2.6362	3.9965	-0.234
C	-3.5682	3.0152	-0.1995
C	-2.838	1.759	-0.0596
C	-3.4792	0.5035	0.0046
C	-2.8247	-0.74	0.0508
C	-3.4373	-2.0286	0.1953
C	-2.4463	-2.9738	0.2119
C	-1.186	-2.3032	0.0786
C	0.0878	-2.8969	0.0749
C	1.3116	-2.1966	0.0185
C	2.6096	-2.8648	-0.0044
C	3.5423	-1.8841	-0.0389
C	2.8098	-0.6213	-0.0545
C	3.4506	0.6364	-0.0747
H	4.484	3.3386	-0.1298
H	2.5529	5.193	-0.1364
H	-2.7983	5.0586	-0.3493
H	-4.6409	3.1154	-0.2803
H	-4.5004	-2.191	0.2893
H	-2.5599	-4.0418	0.321
H	2.7687	-3.9334	0.0056
H	4.6175	-1.9891	-0.0528
C	-0.1572	5.5317	-0.1863
C	0.3038	6.2276	-1.3164
C	-0.663	6.2729	0.8957
C	0.263	7.6184	-1.368
H	0.6865	5.6669	-2.1641
C	-0.7055	7.6621	0.85
H	-1.0174	5.7478	1.7776
C	-0.2426	8.3461	-0.2821
H	0.6156	8.1426	-2.2495
H	-1.0904	8.2376	1.6856
C	4.9513	0.6692	-0.0977
C	5.6476	0.3083	-1.2583
C	5.6677	1.0634	1.0395
C	7.0472	0.3327	-1.3023
H	5.0727	0.011	-2.1276
C	7.0679	1.1016	1.0387
H	5.1088	1.3323	1.9284
C	7.7268	0.7323	-0.1426
H	8.8125	0.7563	-0.1601
C	-4.978	0.472	0.0334
C	-5.6734	0.9678	1.1443
C	-5.6977	-0.0551	-1.0472

C	-7.0725	0.9462	1.195
H	-5.0971	1.3654	1.9715
C	-7.0976	-0.0927	-1.0392
H	-5.1411	-0.4258	-1.9
C	-7.7545	0.4122	0.0921
H	-8.8401	0.3893	0.115
C	0.1257	-4.3946	0.1519
C	0.5902	-5.0319	1.3099
C	-0.3085	-5.1698	-0.9314
C	0.6298	-6.4284	1.4043
H	0.9152	-4.413	2.138
C	-0.2838	-6.5691	-0.8798
H	-0.6577	-4.6566	-1.8198
C	0.1879	-7.1674	0.2974
H	0.2126	-8.2517	0.3544
C	7.8882	1.5232	2.2737
C	8.7569	2.7541	1.9211
C	6.9948	1.897	3.4719
C	8.8065	0.3553	2.7059
H	9.4507	2.544	1.1004
H	8.1311	3.6023	1.6206
H	9.3519	3.0623	2.7896
H	6.3734	1.0549	3.7968
H	7.6219	2.1912	4.3211
H	6.334	2.7404	3.2419
H	9.401	0.6415	3.5822
H	8.2163	-0.5295	2.97
H	9.5026	0.0672	1.9112
C	7.8454	-0.0548	-2.5626
C	8.7759	-1.2476	-2.2375
C	6.9315	-0.4675	-3.7322
C	8.6997	1.1501	-3.0232
H	9.4857	-1.0073	-1.439
H	8.1959	-2.1208	-1.9173
H	9.3557	-1.5316	-3.1243
H	6.2649	0.3471	-4.037
H	7.5435	-0.7356	-4.6008
H	6.3147	-1.3379	-3.4815
H	9.2783	0.888	-3.9176
H	8.0649	2.009	-3.2692
H	9.4075	1.4686	-2.2507
C	-7.9199	-0.6568	-2.2145
C	-8.8466	0.4487	-2.7741
C	-7.0287	-1.1604	-3.366
C	-8.78	-1.8439	-1.7195
H	-9.5421	0.822	-2.0152
H	-8.2627	1.3009	-3.14
H	-9.4421	0.0607	-3.6097
H	-6.3635	-1.9697	-3.0443
H	-7.6571	-1.5514	-4.1741
H	-6.412	-0.358	-3.7863
H	-9.3762	-2.2534	-2.5442
H	-8.1481	-2.6482	-1.3256
H	-9.4721	-1.5444	-0.9255
C	-7.8676	1.4779	2.4036
C	-8.7213	0.3352	3.0032
C	-6.9505	2.0229	3.5152
C	-8.7982	2.6255	1.9442
H	-9.4314	-0.0702	2.2748

H	-8.0861	-0.4898	3.3455
H	-9.2972	0.6998	3.8626
H	-6.3348	2.8586	3.1641
H	-7.5602	2.3895	4.3488
H	-6.2829	1.2489	3.9102
H	-9.375	3.012	2.7934
H	-8.2187	3.4547	1.5223
H	-9.5106	2.2941	1.1814
C	-0.7457	-7.4519	-2.0558
C	-1.9166	-8.3528	-1.596
C	-1.2274	-6.6204	-3.2601
C	0.4299	-8.3409	-2.5268
H	-1.6287	-9.0055	-0.7653
H	-2.7695	-7.7487	-1.2657
H	-2.253	-8.9925	-2.4213
H	-0.4328	-5.9791	-3.6577
H	-1.5454	-7.2906	-4.0668
H	-2.0825	-5.9851	-3.0026
H	0.1153	-8.9786	-3.3621
H	1.2726	-7.7278	-2.8661
H	0.7936	-8.9949	-1.7274
C	1.1308	-7.1616	2.6641
C	2.3402	-8.0533	2.2951
C	1.5762	-6.1876	3.7716
C	-0.0041	-8.0472	3.2316
H	2.0811	-8.8024	1.5396
H	3.1649	-7.4502	1.8983
H	2.7054	-8.5866	3.1814
H	0.7541	-5.5444	4.1051
H	1.9253	-6.7546	4.6421
H	2.401	-5.5452	3.4435
H	0.3392	-8.5801	4.1268
H	-0.8725	-7.4395	3.5104
H	-0.3395	-8.7962	2.5066
C	-0.3106	9.8294	-0.2799
O	-0.7413	10.5073	0.6324
O	0.1663	10.3868	-1.4243
Zn	-0.3032	12.0061	-0.5268
Pt	-0.066	0.6175	-0.0482

P2, Total Energy (excluding Pt and Zn) = -3276.910722 Hartree			
N	1.0724	-1.5214	-0.029
N	1.09	1.4096	0.0265
N	-1.8467	1.5262	-0.0064
N	-1.8624	-1.4056	-0.0211
C	0.7906	-2.869	-0.038
C	2.0541	-3.5469	-0.0505
C	3.0463	-2.6033	-0.04
C	2.4315	-1.3069	-0.0401
C	3.0814	-0.0609	-0.0547
C	2.4374	1.1963	-0.049
C	3.1601	2.4601	-0.1604
C	2.2235	3.4376	-0.1373
C	0.9327	2.7674	-0.0126
C	-0.2924	3.4669	0.036
C	-1.5654	2.8715	0.064
C	-2.8262	3.543	0.1922
C	-3.8166	2.597	0.193
C	-3.2035	1.307	0.066

C	-3.8559	0.0624	0.0502
C	-3.2127	-1.1927	-0.0002
C	-3.9406	-2.458	-0.0374
C	-3.0042	-3.4355	-0.0611
C	-1.7083	-2.7631	-0.055
C	-0.4821	-3.462	-0.057
H	2.1699	-4.6202	-0.0645
H	4.112	-2.7759	-0.0356
H	4.2301	2.5706	-0.2633
H	2.375	4.5043	-0.2171
H	-2.9404	4.6123	0.2867
H	-4.8797	2.7599	0.2873
H	-5.0155	-2.5668	-0.0434
H	-3.1593	-4.5046	-0.0805
C	4.5783	-0.087	-0.0851
C	5.2747	-0.5724	-1.2029
C	5.3297	0.3755	1.0066
C	6.6669	-0.5937	-1.2289
H	4.7152	-0.9344	-2.0609
C	6.7216	0.3517	0.9826
H	4.8124	0.7595	1.8812
C	7.4202	-0.133	-0.1361
H	7.1763	-0.9938	-2.1011
H	7.2746	0.7365	1.8349
C	-0.5195	-4.9625	-0.0846
C	-0.8869	-5.6379	-1.2553
C	-0.1846	-5.6998	1.0583
C	-0.9277	-7.037	-1.3041
H	-1.1373	-5.0471	-2.1287
C	-0.2126	-7.1003	1.0531
H	0.0909	-5.1566	1.9548
C	-0.5866	-7.7379	-0.1384
H	-0.6137	-8.8235	-0.1592
C	-0.2534	4.9654	0.0678
C	0.265	5.6345	1.1847
C	-0.7354	5.7118	-1.0159
C	0.3104	7.0329	1.2382
H	0.6269	5.0382	2.014
C	-0.7056	7.1118	-1.0052
H	-1.1242	5.1751	-1.8735
C	-0.1801	7.7418	0.1321
H	-0.1507	8.8272	0.157
C	-5.3546	0.094	0.1066
C	-6.0283	-0.3397	1.256
C	-6.0943	0.5627	-0.987
C	-7.4264	-0.3145	1.3316
H	-5.4363	-0.6925	2.0923
C	-7.4939	0.6023	-0.9545
H	-5.5535	0.8877	-1.8683
C	-8.1292	0.1596	0.2145
H	-9.2142	0.1847	0.2566
C	0.1433	-7.9427	2.2938
C	1.3395	-8.8673	1.9647
C	0.5326	-7.071	3.503
C	-1.0752	-8.8065	2.6977
H	1.115	-9.5485	1.1373
H	2.2223	-8.2812	1.6845
H	1.6009	-9.4782	2.8375
H	-0.2862	-6.4116	3.812

H	0.7788	-7.7134	4.3561
H	1.4109	-6.45	3.2933
H	-0.8361	-9.4159	3.5779
H	-1.9371	-8.1762	2.9448
H	-1.3784	-9.4864	1.8946
C	-1.3239	-7.8125	-2.5758
C	-2.5668	-8.6858	-2.2813
C	-1.6656	-6.8768	-3.7511
C	-0.1508	-8.7221	-3.0122
H	-2.3786	-9.4084	-1.4803
H	-3.4183	-8.0657	-1.9785
H	-2.858	-9.2491	-3.1765
H	-0.8134	-6.249	-4.0346
H	-1.9422	-7.4731	-4.628
H	-2.5113	-6.22	-3.5183
H	-0.4197	-9.2851	-3.9145
H	0.7427	-8.1282	-3.2362
H	0.1158	-9.4463	-2.2353
C	-1.2172	7.9627	-2.1842
C	-0.0612	8.8326	-2.7327
C	-1.7553	7.0993	-3.3413
C	-2.3634	8.8816	-1.6984
H	0.3405	9.5071	-1.9692
H	0.7633	8.2063	-3.0921
H	-0.4109	9.4482	-3.5706
H	-2.5996	6.475	-3.0275
H	-2.1075	7.7476	-4.1516
H	-0.9813	6.4437	-3.7559
H	-2.7348	9.4986	-2.5258
H	-3.2023	8.291	-1.3124
H	-2.0361	9.5568	-0.9009
C	0.8698	7.7993	2.4528
C	-0.2347	8.7073	3.0441
C	1.3596	6.8551	3.5673
C	2.0657	8.6731	2.0049
H	-0.5983	9.4377	2.3137
H	-1.0929	8.1129	3.3779
H	0.1502	9.2632	3.9079
H	2.1669	6.1995	3.2219
H	1.7487	7.4449	4.405
H	0.5505	6.2257	3.9545
H	2.4724	9.2294	2.8583
H	2.8691	8.054	1.5894
H	1.7765	9.4017	1.2403
C	-8.3386	1.1032	-2.1425
C	-9.1914	2.3142	-1.6952
C	-7.4694	1.5459	-3.3351
C	-9.2735	-0.031	-2.6257
H	-9.8686	2.0569	-0.8741
H	-8.5537	3.1387	-1.356
H	-9.8031	2.6793	-2.5295
H	-6.8594	0.7228	-3.7238
H	-8.1132	1.8936	-4.151
H	-6.7995	2.3713	-3.0687
H	-9.8854	0.312	-3.4691
H	-8.6948	-0.9006	-2.9572
H	-9.9538	-0.3645	-1.835
C	-8.1987	-0.7793	2.5819
C	-9.1381	-1.9489	2.2028

C	-7.2611	-1.2646	3.7038
C	-9.0408	0.3951	3.1348
H	-9.8643	-1.6587	1.4363
H	-8.5668	-2.8006	1.8162
H	-9.6995	-2.2876	3.0823
H	-6.5861	-0.4712	4.044
H	-7.8551	-1.5852	4.5672
H	-6.6519	-2.1185	3.3866
H	-9.601	0.078	4.023
H	-8.3991	1.2364	3.4205
H	-9.764	0.7618	2.3987
C	8.9031	-0.1565	-0.1624
C	9.6102	0.1152	-1.3476
C	9.6431	-0.4509	0.9979
C	11.0004	0.0939	-1.377
H	9.0623	0.3724	-2.2493
C	11.0319	-0.4723	0.9746
H	9.1203	-0.6908	1.9191
C	11.7241	-0.2004	-0.2131
H	11.5297	0.3141	-2.2975
H	11.6019	-0.7075	1.8674
C	13.2073	-0.237	-0.1839
O	13.8806	-0.4865	0.7969
O	13.7716	0.0416	-1.3891
Pt	-0.3805	0.0089	-0.0131
Zn	15.4049	-0.1921	-0.3665

P3, Total Energy (excluding Pt and Zn) = -3507.968451 Hartree			
N	-0.0221	-1.5017	-0.0024
N	-0.0414	1.4291	0.045
N	-2.9791	1.509	-0.0117
N	-2.9582	-1.4226	-0.0179
C	-0.287	-2.8527	-0.0099
C	0.9851	-3.5148	-0.0112
C	1.9653	-2.5587	0.0043
C	1.3344	-1.2702	-0.0038
C	1.9692	-0.0165	-0.017
C	1.3093	1.2324	-0.0197
C	2.017	2.5048	-0.1286
C	1.0682	3.4706	-0.115
C	-0.2151	2.7847	0.001
C	-1.4493	3.469	0.0375
C	-2.715	2.858	0.0566
C	-3.9851	3.5141	0.1718
C	-4.9637	2.556	0.1674
C	-4.3337	1.2733	0.0499
C	-4.9703	0.0206	0.0327
C	-4.3112	-1.2266	-0.0084
C	-5.0229	-2.5009	-0.047
C	-4.0743	-3.4668	-0.0602
C	-2.7869	-2.7782	-0.0463
C	-1.5521	-3.4617	-0.0368
H	1.1143	-4.5866	-0.0217
H	3.0331	-2.7175	0.0168
H	3.0863	2.6281	-0.2233
H	1.2069	4.539	-0.1961
H	-4.1133	4.5823	0.2616
H	-6.0294	2.7061	0.2521
H	-6.0963	-2.6232	-0.0611

H	-4.2159	-4.5377	-0.0772
C	3.4666	-0.0242	-0.0367
C	4.1771	-0.5023	-1.1487
C	4.2048	0.4489	1.0594
C	5.5698	-0.5074	-1.1641
H	3.6283	-0.8723	-2.0102
C	5.5972	0.4436	1.0443
H	3.6768	0.8277	1.9299
C	6.3105	-0.0349	-0.0677
H	6.0901	-0.9033	-2.0318
H	6.1392	0.8378	1.8994
C	-1.5705	-4.9626	-0.0601
C	-1.9235	-5.6461	-1.2306
C	-1.2323	-5.6924	1.0866
C	-1.9468	-7.0457	-1.2753
H	-2.1768	-5.061	-2.107
C	-1.2429	-7.0931	1.0855
H	-0.9682	-5.143	1.9829
C	-1.6029	-7.7389	-0.1058
H	-1.6164	-8.8247	-0.1235
C	-1.4294	4.968	0.0647
C	-0.9316	5.6471	1.1848
C	-1.9091	5.7047	-1.0266
C	-0.9048	7.0461	1.2343
H	-0.5709	5.0581	2.0199
C	-1.8974	7.105	-1.0201
H	-2.2819	5.1603	-1.8864
C	-1.3925	7.7453	0.1207
H	-1.3775	8.831	0.1425
C	-6.4698	0.0338	0.0764
C	-7.1479	-0.4043	1.2216
C	-7.2059	0.4895	-1.025
C	-8.5467	-0.3962	1.2853
H	-6.5587	-0.7468	2.0641
C	-8.6062	0.5118	-1.0045
H	-6.6618	0.818	-1.9029
C	-9.2459	0.0653	0.1606
H	-10.3314	0.0771	0.1935
C	-0.8831	-7.9273	2.3306
C	0.3256	-8.8386	2.0105
C	-0.5103	-7.0474	3.5391
C	-2.0933	-8.8043	2.7312
H	0.1134	-9.5249	1.184
H	1.2029	-8.2429	1.7329
H	0.5898	-9.4438	2.8864
H	-1.3385	-6.397	3.842
H	-0.2605	-7.6842	4.3953
H	0.3614	-6.4164	3.3317
H	-1.8514	-9.4082	3.6145
H	-2.9638	-8.1836	2.972
H	-2.3843	-9.4902	1.9286
C	-2.3271	-7.8298	-2.5466
C	-3.5602	-8.7179	-2.2555
C	-2.6751	-6.902	-3.7263
C	-1.1406	-8.7258	-2.9748
H	-3.3668	-9.4357	-1.4513
H	-4.421	-8.1078	-1.9587
H	-3.84	-9.2875	-3.1503
H	-1.8295	-6.2643	-4.0077

H	-2.9401	-7.5043	-4.6027
H	-3.53	-6.2551	-3.4993
H	-1.3979	-9.2947	-3.8767
H	-0.2536	-8.1213	-3.1962
H	-0.8686	-9.4443	-2.1944
C	-2.4074	7.9454	-2.2074
C	-1.2578	8.8306	-2.7448
C	-2.9193	7.0713	-3.3682
C	-3.5724	8.8487	-1.7374
H	-0.875	9.513	-1.9788
H	-0.4202	8.2155	-3.0929
H	-1.6068	9.4388	-3.5885
H	-3.7584	6.4361	-3.0627
H	-3.2708	7.7123	-4.1846
H	-2.1313	6.4255	-3.7716
H	-3.9432	9.4581	-2.5707
H	-4.4071	8.2469	-1.3596
H	-3.2643	9.5305	-0.9379
C	-0.3688	7.8236	2.4524
C	-1.4915	8.719	3.0286
C	0.1207	6.8893	3.5754
C	0.8205	8.7113	2.0149
H	-1.8565	9.4422	2.2917
H	-2.3455	8.1146	3.355
H	-1.1233	9.2828	3.8946
H	0.9402	6.2432	3.241
H	0.4927	7.4867	4.4155
H	-0.6844	6.2506	3.9556
H	1.2107	9.2755	2.871
H	1.6364	8.1015	1.6103
H	0.5304	9.4338	1.2449
C	-9.4469	0.9981	-2.2014
C	-10.3181	2.2003	-1.7658
C	-8.5732	1.4471	-3.3884
C	-10.3638	-0.1491	-2.6882
H	-10.9988	1.9377	-0.9492
H	-9.6933	3.0337	-1.4246
H	-10.9273	2.5547	-2.6064
H	-7.9499	0.63	-3.7689
H	-9.2142	1.7839	-4.2109
H	-7.9156	2.2815	-3.1194
H	-10.9726	0.1832	-3.5381
H	-9.7718	-1.0129	-3.0115
H	-11.0467	-0.488	-1.9021
C	-9.3239	-0.8662	2.5306
C	-10.2457	-2.0485	2.1475
C	-8.39	-1.3364	3.6621
C	-10.1849	0.2996	3.0723
H	-10.9688	-1.7698	1.3739
H	-9.6607	-2.8944	1.7687
H	-10.8104	-2.3912	3.0234
H	-7.7277	-0.5337	4.0053
H	-8.9873	-1.6615	4.5214
H	-7.7677	-2.1837	3.3528
H	-10.7487	-0.0213	3.9569
H	-9.5559	1.1496	3.3605
H	-10.9063	0.655	2.329
C	7.7936	-0.0399	-0.084
C	8.5103	0.2305	-1.2623

C	8.5342	-0.3148	1.0783
C	9.9011	0.2245	-1.2782
H	7.9705	0.4833	-2.1704
C	9.925	-0.3175	1.0638
H	8.0128	-0.5634	1.9983
C	10.641	-0.0489	-0.1152
H	10.4221	0.4728	-2.1986
H	10.4645	-0.5685	1.9728
C	12.1233	-0.0536	-0.1311
C	12.8336	-0.5284	-1.2487
C	12.8611	0.4168	0.9714
C	14.2241	-0.5337	-1.2686
H	12.2874	-0.9226	-2.1005
C	14.25	0.4121	0.9576
H	12.3366	0.8144	1.8352
C	14.9453	-0.0629	-0.1626
H	14.7555	-0.9111	-2.1353
H	14.8182	0.7825	1.8046
C	16.4286	-0.0449	-0.1263
O	17.0997	0.3519	0.8064
O	16.9959	-0.5267	-1.2641
Pt	-1.5477	-0.0389	-0.1218
Zn	18.648	-0.1161	-0.3005

References:

1. P. Mishra, J. P. Hill, S. Vijayaraghavan, W. V. Rossom, S. Yoshizawa, M. Grisolia, J. Echeverria, T. Ono, K. Ariga, T. Nakayama, C. Joachim and T. Uchihashi, *Nano Lett.*, 2015, **15**, 4793–4798.
2. U. Ryde, *Biophys. J.*, 1999, **77**, 2777–2787.
3. Y. Zorlu, L. Wagner, P. Tholen, M. M. Ayhan, C. Bayraktar, G. Hanna, A. O. Yazaydin, Ö. Yavuzçetin and G. Yücesan, *Adv. Opt. Mater.*, 2022, **10**, 2200213.
4. B. Norden, G. Lindblom and I. Jonas, *J. Phys. Chem.*, 1977, **81**, 2086–2093.
5. B. F. Kim and J. Bohandy, .
6. J. Mårtensson, *Chem. Phys. Lett.*, 1994, **229**, 449–456.